Function-Valued Mappings, Total Variation and Compressed Sensing for diffusion MRI

O. Michailovich[1], D. La Torre[2], and Edward R. Vrscay[1]

[1] Department of Electrical and Computer Engineering,
University of Waterloo, Waterloo, Ontario, Canada N2L 3G1
[2] Department of Economics, Business and Statistics,
University of Milan, Italy
[3] Department of Applied Mathematics,
University of Waterloo, Waterloo, Ontario, Canada N2L 3G1

Abstract. Being the only imaging modality capable of delineating the anatomical structure of the white matter, diffusion magnetic resonance imaging (dMRI) is currently believed to provide a long-awaited means for early diagnosis of various neurological conditions as well as for interrogating the brain connectivity. Despite substantial advances in practical use of dMRI, a solid mathematical platform for modelling and treating dMRI signals still seems to be missing. Accordingly, in this paper, we show how a Hilbert space of $\mathbb{L}^2$-valued mappings $u : X \to \mathbb{L}^2(\mathbb{S}^2)$, with X being a subset of $\mathbb{R}^3$ and $\mathbb{L}^2(\mathbb{S}^2)$ being the set of squared-integrable functions supported on the unit sphere $\mathbb{S}^2$, provides a natural setting for a specific example of dMRI, known as high-angular resolution diffusion imaging. The proposed formalism is also shown to provide a basis for image processing schemes such as total variation minimization. Finally, we discuss a way to amalgamate the proposed models with the tools of compressed sensing to achieve a close-to-perfect recovery of diffusion signals from a minimal number of their discrete measurements. The main outcomes of this paper are supported by a series of experimental results.

Keywords: $\mathbb{L}^2$-valued functions, image analysis, diffusion MRI and compressed sensing.

1 Introduction

Made possible by the physical phenomenon of nuclear magnetic resonance, magnetic resonance imaging (MRI) has long become one of the most powerful and accurate tools of medical diagnostic imaging. However, it is only with the advent of diffusion MRI (dMRI) that scientists have been able to perform quantitative measurements of the diffusivity of the white matter, based on which its structural delineation has become possible [1,2]. The current paper focuses on a specific instance of dMRI known as *high angular resolution diffusion imaging* (HARDI), which excels in delineation of the orientational structure of crossing fibre bundles in the white matter of the brain [3,4,5]. At the practical level, for each fixed position $x \in \mathbb{R}^3$ and orientation $s \in \mathbb{S}^2$, HARDI provides a measurement that

A. Campilho and M. Kamel (Eds.): ICIAR 2012, Part II, LNCS 7325, pp. 286–295, 2012.

quantifies the apparent diffusivity of water molecules along the direction defined by s. Therefore, a HARDI signal u measured at position x, can be assumed to be a square-integrable function supported over $\mathbb{S}^2$. Formally, $u(s|x) \in \mathbb{L}^2(\mathbb{S}^2)$.

In the majority of recent works which address the problem of reconstruction of HARDI signals from their discrete measurements, HARDI signals $u(s|x)$ are processed at each given x independently of their values at neighbouring spatial locations [3,6,7,8]. Ignoring the spatial regularity of $u(s|x)$ is a serious omission, which needs to be rectified via appropriate extensions of existing models. In this regard, we would like to mention the work of Duits *et. al.* [9], in which HARDI signals are spatially regularized by means of convolution-type operators applied over the group of rigid motions in $\mathbb{R}^3$.

In this work, a different route to description of the HARDI signals is taken by means of a novel mathematical formulation. In particular, we consider HARDI signals to be $\mathbb{L}^2$-valued maps $u : X \subset \mathbb{R}^3 \to \mathbb{L}^2(\mathbb{S}^2)$, which represents an extension of work in [10] and [11]. We establish the existence of a Gateaux derivative on this space, thus providing a rigorous definition of total variation which will be employed in our image processing scheme. Finally, we show how the proposed constructions can be used to recover HARDI signals from a minimal set of their discrete measurements using the tools of compressed sensing [12,13].

2 A Complete Metric Space (Y, d_Y) of $\mathbb{L}^2$-Valued Mappings

First, we list the following ingredients for our formalism:

The base space X: the compact support of HARDI signals. We let d_X denote the metric on this space which, for the sake of convenience, we consider to be $X = [0, 1]^3$. (In practical computations, X will have to be replaced by its discrete counterpart. We shall address this matter later.)

The range space $\mathbb{L}^2(\mathbb{S}^2)$: the space of all $\mathbb{L}^2$-integrable functions supported over $\mathbb{S}^2$. $\mathbb{L}^2(\mathbb{S}^2)$ is a Hilbert space with the standard definition of the inner product, *viz.*

$$\langle f, g\rangle_{\mathbb{L}^2} = \int_{\mathbb{S}^2} f(s)\, g^*(s)\, d\eta(s), \quad \forall f, g \in \mathbb{L}^2(\mathbb{S}^2), \tag{1}$$

where $d\eta$ denotes the surface element of $\mathbb{S}^2$ and the asterisk stands for complex conjugation.

Now, let (Y, d_Y) be the set of all function-valued mappings from $X \in \mathbb{R}^3$ to $\mathbb{L}^2(\mathbb{S}^2)$. Given a signal $u \in Y$, its value $u(x)$ at a particular location $x \in X$ will be an element of the space $\mathbb{L}^2(\mathbb{S}^2)$. To define the metric d_Y on Y, we first endow the latter with an inner product

$$\langle u, v\rangle_Y = \int_X \langle u(x), v(x)\rangle_{\mathbb{L}^2}\, dx, \quad u, v \in Y \tag{2}$$

and the related norm

$$\|u\|_Y^2 = \int_X \|u(x)\|_{\mathbb{L}^2}^2 \, dx, \quad u, v \in Y, \tag{3}$$

so that $d_Y(u,v) = \|u - v\|_Y$, $\forall u, v \in Y$. Subsequently, redefining Y as

$$Y = \big\{u : X \to \mathbb{L}^2(\mathbb{S}^2) \mid \|u\|_Y < +\infty\big\} \tag{4}$$

makes the inner product space (Y, d_Y) into a Hilbert space. Note that the completeness of (Y, d_Y) follows directly from the completeness of $\mathbb{L}^2(X \times \mathbb{S}^2)$ which is, in turn, isomorphic to (Y, d_Y).

Our next step is to find a way to express the elements of (Y, d_Y) in terms of basis functions. To this end, let $\{\psi_i\}_{i\in\mathcal{I}}$ be a frame for $\mathbb{L}^2(\mathbb{S}^2)$, which is defined as a collection of functions obeying [14]

$$A \, \|f\|_{\mathbb{L}^2} \le \sum_{i\in\mathcal{I}} |\langle f, \psi_i\rangle_{\mathbb{L}^2}|^2 \le B \, \|f\|_{\mathbb{L}^2}, \quad \forall f \in \mathbb{L}^2(\mathbb{S}^2), \tag{5}$$

for some frame bounds $0 < A, B < \infty$. Accordingly, any $f \in \mathbb{L}^2(\mathbb{S}^2)$ can now be expanded in terms of $\{\psi_i\}_{i\in\mathcal{I}}$ as given by

$$f = \sum_{i\in\mathcal{I}} c_i \psi_i \quad \text{with} \quad c_i = \langle f, \tilde{\psi}_i\rangle_{\mathbb{L}^2}, \tag{6}$$

where $\{\tilde{\psi}_i\}_{i\in\mathcal{I}}$ denotes the canonical dual frame of $\{\psi_i\}_{i\in\mathcal{I}}$ [15].

The frame $\{\psi_i\}_{i\in\mathcal{I}}$ can be used to expand the function-valued mappings in Y according to

$$u(x) = \sum_{i\in\mathbb{Z}} c_i(x) \psi_i, \tag{7}$$

where

$$c_i(x) = \langle u(x), \tilde{\psi}_i\rangle_{\mathbb{L}^2}, \quad \forall x \in X. \tag{8}$$

Finally, in order to be able to control the spatial regularity of HARDI signals, the Gateaux derivative of $u : X \to \mathbb{L}^2(\mathbb{S}^2)$ can be defined as follows. First, let X^o be an open set containing X, and u^o be a continuous extension[1] of u to the maps of the form $X^o \to \mathbb{L}^2(\mathbb{S}^2)$. Then, for an arbitrary location $x \in X$ and direction $d \in \mathbb{R}^3$ (with $\|d\| = 1$), we say that $Du(x,d)$ is the Gateaux derivative of u at x in the direction d if and only if

$$\lim_{t\downarrow 0} \left\| \frac{u^o(x + t\,d) - u(x)}{t} - Du(x,d) \right\|_{\mathbb{L}^2} = 0. \tag{9}$$

Let us notice that the above difference is well defined in the Hilbert space $\mathbb{L}^2(\mathbb{S}^2)$. Furthermore, for each Gateaux differentiable test function $\phi : X \to \mathbb{L}^2(\mathbb{S}^2)$ with a compact support in X, it is true that [16]

$$\int_X \langle Du(x,d), \phi(x)\rangle dx = -\int_X \langle u(x), D\phi(x,d)\rangle dx. \tag{10}$$

[1] In image processing, a typical way to construct such an extension is by using, e.g., reflective boundary conditions.

For any $u \in Y$ with $Du(x,d) \in \mathbb{L}^2(\mathbb{S}^2)$, the definition of the Gateaux derivative in (9) and (10) allows us to define its *total variation semi-norm* as

$$\|u\|_{TV} = \sum_{l=1}^{3} \int_X \|Du(x,d_l)\|_{\mathbb{L}^2}\, dx, \tag{11}$$

where $\{d_l\}_{l=1}^3$ defines the canonical coordinate system in $\mathbb{R}^3$. From now on, we will restrict the signals of interest $u \in Y$ to be members of the following space

$$\mathcal{B} = \Big\{u : X \to \mathbb{L}^2(\mathbb{S}^2) \mid Du(x,d_l) \in \mathbb{L}^2(\mathbb{S}^2)\ \forall x,l,\ \|u\|_Y + \|u\|_{TV} < +\infty\Big\}. \tag{12}$$

Lemma 1. *$\mathcal{B}$ is a Banach space.*

Proof. The proof follows from the completeness of (Y, d_Y) as well as the following series of arguments. First, let $\{u_n\}$ be a Cauchy sequence in $\mathcal{B}$. Then, $\{u_n\}$ is a Cauchy sequence in Y which is complete and, therefore, $u_n \to u$ for some $u \in Y$. On the other hand, $\{Du_n\}$ is a Cauchy sequence in Y as well and therefore it has a limit L in Y. Finally, by Theorem 1.1 of [17], $L = Du$, thereby implying $u \in \mathcal{B}$.

3 Application to Diffusion MRI

We first outline the most important aspects of HARDI which will motivate the formalism of the previous section. Specifically, a principal quantities analyzed in diffusion MRI is the average diffusion propagator $p(r) : \mathbb{R}^3 \to \mathbb{R}^+$. This function quantifies the ensemble-averaged probability of a water molecule to undergo spatial translation by r at experimental time τ. In HARDI, a full reconstruction of $p(r)$ is superseded by recovering its related *orientation probability distribution function* (OPDF) $\psi(u) : \mathbb{S}^2 \to \mathbb{R}^+$, which is defined according to

$$\Psi(s) = \int_0^\infty p(\alpha\, s)\, \alpha^2\, d\alpha, \quad s \in \mathbb{S}^2. \tag{13}$$

The primary value of OPDF $\Psi(s)$ is in its ability to quantity the likelihood with which local diffusion is expected to occur along the spatial orientation s. At the technical level, the OPDF $\Psi(s)$ can be closely approximated by applying the Funk-Radon transform [18] to its associated diffusion signal $u(s)$ measured over a spherical shell in the q-space [3]. Thus, to compute $\Psi(s)$, it is imperative to find an accurate scheme for reconstruction of $u(s)$ from its discrete measurements. Our solution to this problem is presented next.

3.1 Measurement Model for HARDI Signals

Let $u(x)$ be a HARDI signal corresponding to the spatial location $x \in X$. Then, given a set of K diffusion-encoding direction $\{s_k\}_{k=1}^K$, their corresponding sampling function are defined to be $\phi_k = \delta(1 - s_k \cdot s)$, where δ is the Dirac delta function and the dot stands for the Euclidean dot product. Consequently, HARDI measurements can be described as

$$y_k(x) = \langle u(x), \phi_k \rangle_{\mathbb{L}^2} + e_k(x), \quad k = 1, 2, \ldots, K, \ \forall x \in X, \tag{14}$$

where $e_k(x)$ is added to account for both measurement imperfections and noises. Note that, for each k, $y_k(x)$ is a scalar-valued function from X to $\mathbb{R}$. In diffusion MRI, this function is commonly referred to as a diffusion-encoded image associated to direction s_k. The frame coefficients $c(x)$ corresponding to different $u(x)$, on the other hand, can be amalgamated into a vector-valued map $c : X \to \ell_2(\mathcal{I}) : x \mapsto c(x)$. Furthermore, since the frame coefficients c uniquely define u through (7), the problem of recovering u from its discrete and noisy samples can be reduced to an equivalent problem of estimating an optimal c.

In practical computations, the infinite-dimensional set of frame indices $\mathcal{I}$ has to be replace by a finite-dimensional set $\mathcal{I}_M \subset \mathcal{I}$ of cardinality $M < \infty$. One way to do that would be, e.g., by solving

$$\inf_{\mathcal{I}_M \subset \mathcal{I}} \sup_{u \in \mathcal{B}} \int_X \Big\| u(x) - \sum_{i \in \mathcal{I}_M} \langle u(x), \tilde{\psi} \rangle \, \psi \Big\|_{\mathbb{L}^2} dx, \tag{15}$$

where the minimization is carried out over all subsets of $\mathcal{I}$ of cardinality M. The optimal result thus obtained defines the subspace $\overline{\mathrm{Span}\{\psi_i\}_{i \in \mathcal{I}_M}}^{\mathbb{L}^2}$ which can be used for approximation of functions from Y. Specifically, let $\mathcal{U}$ be a *synthesis* operator defined as

$$\mathcal{U} : \ell_2(\mathcal{I}_M) \to Y : c(x) \mapsto \mathcal{U}\{c\}(x) = \sum_{i \in \mathcal{I}_M} c_i(x) \psi_i, \ \forall x \in X. \tag{16}$$

Then, given a noisy observation y of u, i.e. $y = u + e$ with $\epsilon = \|e\|_Y^2 < \|u\|_Y^2$, the optimal frame coefficients c could be found as a solution to

$$\inf_c \left\{ \frac{1}{2} \left\| y - \mathcal{U}\{c\} \right\|_Y^2 + \lambda \left\| \mathcal{U}\{c\} \right\|_{TV} + \mu \left\| c \right\|_1 \right\}, \tag{17}$$

where $\lambda, \mu > 0$ are regularization parameters, and the ℓ_1-norm of c is defined in the standard way as[2]

$$\|c\|_1 = \int_X \sum_{i \in \mathcal{I}_M} |c_i(x)| \, dx < +\infty. \tag{18}$$

The incorporation of the ℓ_1-norm $\|c\|_1$ into the minimization functional of (17) is not accidental. Among all possible solutions satisfying $\left\| y - \mathcal{U}\{c\} \right\|_Y^2 \leq \epsilon$, minimizing $\|c\|_1$ will favour the ones with a maximal degree of sparsity [19]. In the case when the number of measurements K is much less than M, the sparsity constraint forms a fundamental premise of the theory of compressive sensing (CS) [12,13], based on which a stable approximation of u becomes possible. In the next section, more details on the practical implementation of the reconstruction scheme of (17) are provided.

[2] Note that the norm is well defined due to the finiteness of $\mathcal{I}_M$ and the compactness of X.

3.2 Compressed Sensing of HARDI Data

In practice, HARDI data is discretized both in the spatial and diffusion domains. Let $\Omega_d \subset X$ be a discrete rectangular lattice in X, to which the spatial coordinate x will be restricted from now on. Then, for each $x \in \Omega_d$, HARDI acquisition yields a vector of K values which characterize the apparent water diffusion in the spatial directions $\{s_k\}_{k=1}^K$. Assuming the lattice Ω_d has the size of $N \times M \times L$ points, it is convenient to represent HARDI signals by means of $N \times M \times L \times K$ discrete, real-valued arrays. Consequently, in what follows, the HARDI signal $\bar{u}$ is considered to be a member of $\mathbb{R}^{N\times M\times L\times K}$ (where the bar is added to distinguish between discrete quantities and their continuous counterparts).

Switching to the discrete setting necessitates finding finite dimensional counterparts of the norms in (3) and (11), as well as of the linear expansion in (7). Indexing the elements of $\bar{u}$ by quadruples (i, j, l, k) and using the Einstein summation convention, the norm (3) is transformed into

$$\|\bar{u}\|_{Y,d} = \sqrt{\bar{u}^{ijlk}\, \bar{u}_{ijlk}}, \tag{19}$$

where the summation goes over the indices appearing repetitively in the superscript and subscript positions.

Similarly, let Δ_1, Δ_2 and Δ_3 denote the operators of partial differences taken in the direction of i, j and l indices, respectively. Then, a discrete equivalent of (11) can be expressed as given by

$$\|\bar{u}\|_{TV,d} = \sum_{n=1}^{3} 1^{ijl} \sqrt{1^k \left[(\Delta_n \bar{u})_{ijlk}\right]^2}, \tag{20}$$

where 1 stands for an appropriately-sized array of ones (so that $1^k \bar{u}_{ijlk}$ sums the values of $\bar{u}$ along the direction of its k-th index).

In a manner similar to handling $\bar{u}$, the frame coefficients $\bar{c}$ can be stored and manipulated as $N \times M \times L \times M$ arrays, whose ℓ_1-norm can be defined as

$$\|\bar{c}\|_{1,d} = \mathrm{sign}(\bar{c}^{ijlm})\, \bar{c}_{ijlm}, \tag{21}$$

Finally, let $U \in \mathbb{R}^{K\times M}$ be a matrix whose columns are formed by the values of $\{\psi_i\}_{i\in\mathcal{I}_M}$ evaluated at diffusion-encoding directions $\{s_k\}_{k=1}^K$. With a slight abuse of notations, we denote by U a linear map from $\mathbb{R}^{N\times M\times L\times M}$ to $\mathbb{R}^{N\times M\times L\times K}$ which relates $\bar{c}$ and $\bar{u}$ according to

$$\bar{u}^{ijlk} = U^k_m\, \bar{c}^{ijlm}. \tag{22}$$

Subsequently, using the discrete definitions above, the minimization problem (17) can be transformed into its discretized equivalent as given by

$$\min_{\bar{c}} \left\{ \frac{1}{2} \left\| \bar{y} - U\{\bar{c}\} \right\|^2_{Y,d} + \lambda \left\| U\{\bar{c}\} \right\|_{TV,d} + \mu \left\| \bar{c} \right\|_{1,d} \right\}. \tag{23}$$

Note that the minimization functional in (23) is strictly convex, and hence the problem admits a unique global minimizer $\bar{c}_{opt}$.

The problem (23) can be solved as follows. First, it is cast into an equivalent constrained form

$$\min_{\bar{c},\bar{u}} \left\{ \frac{1}{2} \|\bar{y} - \bar{u}\|_{Y,d}^2 + \lambda \|\bar{u}\|_{TV,d} + \mu \|\bar{c}\|_{1,d} \right\}, \text{ s.t. } U\{\bar{c}\} = \bar{u}, \tag{24}$$

which can be solved using Bregman's algorithm [20], supplemented by alternate direction method of multipliers (ADMM) [21]. For the reason of space, a complete derivation of the optimization procedure is omitted here. It should be mentioned, however, that the use of ADMM allows one to split the solution of (24) into a sequence of easily computable proximity operations, which makes the resulting algorithm particularly attractive from the practical point of view.

4 Experimental Results

The upper left subplot of Fig. 1 shows the glyphs of OPDFs [3] corresponding to simulated HARDI signals. The signals were simulated according to the multimodal Gaussian model of [3,7,5]. Note that the resulting field of OPDFs is supposed to mimic the structure of two crossing fibres, with an additional diffusion component added in the posterior-anterior direction at every x.

The simulated signals were sampled using $K = 16$ diffusion orientations and subsequently contaminated by Rician noise giving rise to signal-to-noise ratio of 18 dB. The resulting data set was used to recover the original HARDI signals and their associated ODFs using the proposed reconstruction approach, which is referred to below as RDG-TV. The algorithm was applied with the values of λ and μ set to be equal to 0.03 and 0.05, respectively.

To complete the description of the experimental setup, the frame $\{\psi_i\}_{i\in\mathcal{I}_M}$ needs to be specified. In this work, we used the frame of *spherical ridgelets*, which were constructed in [22] as a tool for sparse representation of HARDI signals. It is worthwhile noting that it takes only 6-8 ridgelets on average to represent HARDI signals with a precision exceeding the precision of their approximation using 45 spherical harmonics. This fact characterizes the frame of spherical ridgelets as a perfect candidate to be used in CS-based reconstruction of HARDI signals.

For the sake of comparison, two alternative reconstruction methods were used. The first was obtained from RDG-TV by setting $\mu = 0$, which neglects spatial-domain regularization. The resulting algorithm is referred to below as RDG-CS. The second reference method was obtained from RDG-CS by replacing the spherical ridgelets by the basis of spherical harmonics of the eighth order inclusive. The resulting method is referred to below as SH8-CS.

The reconstruction results obtained by all the methods under comparison are shown in Fig. 1. It is easy to see that the estimate computed using the SH8-CS method has the poorest quality of all, which is a direct consequence of the inability of spherical harmonics to sparsely represent HARDI signals. A much more accurate result is achieved by RDG-CS, although some inaccuracies are still noticeable in the central part of the phantom. The reconstruction obtained by the RDG-TV method is obviously of superior quality compared to the alternative approaches.

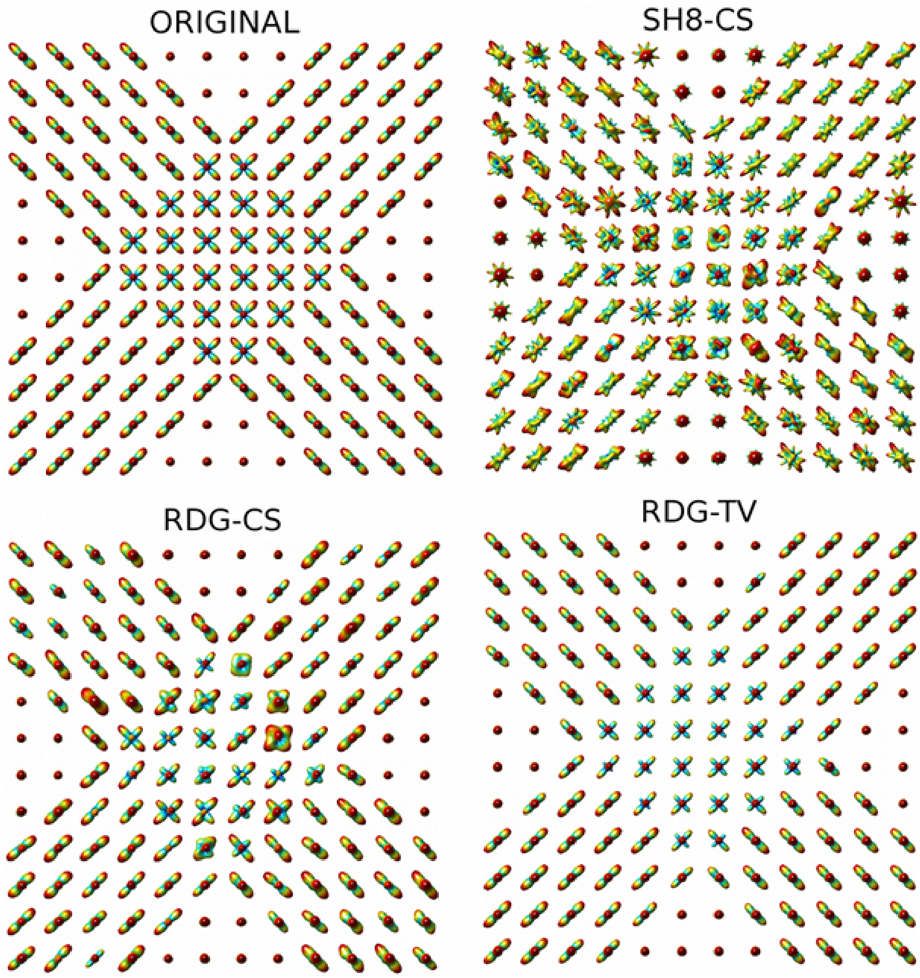

Fig. 1. Estimates of HARDI signals obtained by different methods under comparison

5 Concluding Remarks

In this paper, we have shown how the Hilbert space (Y, d_Y) of function-valued mappings from $X \subset \mathbb{R}^3$ to $\mathbb{L}^2(\mathbb{S}^2)$ can be used to formalize some problems related to the field of diffusion MRI. In particular, the proposed formalism allows one to regularize the spatial behaviour of HARDI signals, which, in combination with their sparse representation in the domain of spherical ridgelet transform, makes it possible to accurately and stably recover the signals from as few as 16 samples per spatial location. Taking into the consideration the fact that the majority of existing HARDI techniques require from 80 to 120 samples per spatial location, the proposed reconstruction framework can be used to substantially reduce the acquisition requirements of HARDI, which are known to be its major bottleneck.

Acknowledgements. This work has been supported in part by Discovery Grants (ERV and OM) from the Natural Sciences and Engineering Research Council of Canada (NSERC).

References

1. Bihan, D.L., Breton, E., Lallemand, D., Grenier, P., Cabanis, E., Laval-Jeantet, M.: MR imaging of intravoxel incoherent motions: Application to diffusion and perfusion in neurological disorders. Radiology 161, 401–407 (1986)
2. Basser, P.J., Mattiello, J., LeBihan, D.: MR diffusion tensor spectroscopy and imaging. Biophys. J. 66(1), 259–267 (1994)
3. Tuch, D.S.: Q-ball imaging. Magnetic Resonance in Medicine 52, 1358–1372 (2004)
4. Anderson, A.W.: Measurement of fiber orientation distributions using high angular resolution diffusion imaging. Magnetic Resonance in Medicine 54, 1194–1206 (2005)
5. Descoteaux, M., Angelino, E., Fitzgibbons, S., Deriche, R.: Apparent diffusion coefficients from high angular resolution diffusion images: Estimation and applications. Magnetic Resonance in Medicine 56(2), 395–410 (2006)
6. Descoteaux, M., Angelino, E., Fitzgibbons, S., Deriche, R.: Regularized, fast, and robust analytical Q-ball imaging. Magnetic Resonance in Medicine 58, 497–510 (2007)
7. Alexander, D.C.: Multiple-fiber reconstruction algorithms for diffusion MRI. Annals of the New York Academy of Science 1064, 113–133 (2005)
8. Landman, B.A., Wan, H., Bogovic, J.A., Bazin, P.L., Prince, J.L.: Resolution of crossing fibers with constrained compressed sensing using traditional Diffusion Tensor MRI. In: Proceedings of SPIE, Medical Imaging, San Diego, CA (February 2010)
9. Duits, R., Franken, E.: Left-invariant diffusions on the space of positions and orientations and their application to crossing-preserving smoothing of hardi images. Int. J. Comput. Vis. (2010), doi:10.1007/s11263-010-0332-z
10. La Torre, D.L., Vrscay, E.R., Ebrahimi, M., Barnsley, M.F.: Measure-valued images, associated fractal transforms and the self-similarity of images. SIAM Journal of Imaging Sciences 2(2), 470–507 (2009)
11. La Torre, D.L., Vrscay, E.R.: Random measure-valued image functions, fractal transforms and self-similarity. Applied Mathematics Letters 24, 1405–1410 (2011)
12. Candes, E., Romberg, J., Tao, T.: Stable signal recovery from incomplete and inaccurate measurements. Communications on Pure and Applied Mathematics 59(8), 1207–1221 (2006)
13. Donoho, D.: Compressed sensing. IEEE Trans. Inform. Theory 52(4), 1289–1306 (2006)
14. Duffin, R.J., Schaeffer, A.C.: A class of nonharmonic Fourier series. Trans. Amer. Math. Soc. 72(2), 341–366 (1952)
15. Christensen, O.: Frames and bases: An introductory course. Birkhäuser (2008)
16. Guoju, Y., Congxin, W., Yee, L.P.: Integration by parts for the Denjoy-Bochner integral. Southeast Asian Bulletin of Mathematics 26, 693–700 (2002)
17. Knapp, A.W.: Advanced real analysis. Birkhäuser (2005)
18. Groemer, H.: Geometric applications of Fourier series and spherical harmonics. Cambridge University Press (1996)

19. Donoho, D.L., Elad, M., Temlyakov, V.N.: Stable recovery of sparse overcomplete representations in the presence of noise. IEEE Trans. Inform. Theory 52(1), 6–18 (2006)
20. Bregman, L.M.: A relaxation method for finding a common point of convex sets and its application to the solution of problems in convex programming. USSR Computational Mathematics and Mathematical Physics (7), 200–217 (1967)
21. Eckstein, J., Bertsekas, D.: On the Douglas-Rachford splitting method and the proximal point algorithm for maximal monotone operators. Mathematical Programming (55) (1992)
22. Michailovich, O., Rathi, Y.: On approximation of orientation distributions by means of spherical ridgelets. IEEE Trans. Image Process. 19(2), 461–477 (2010)